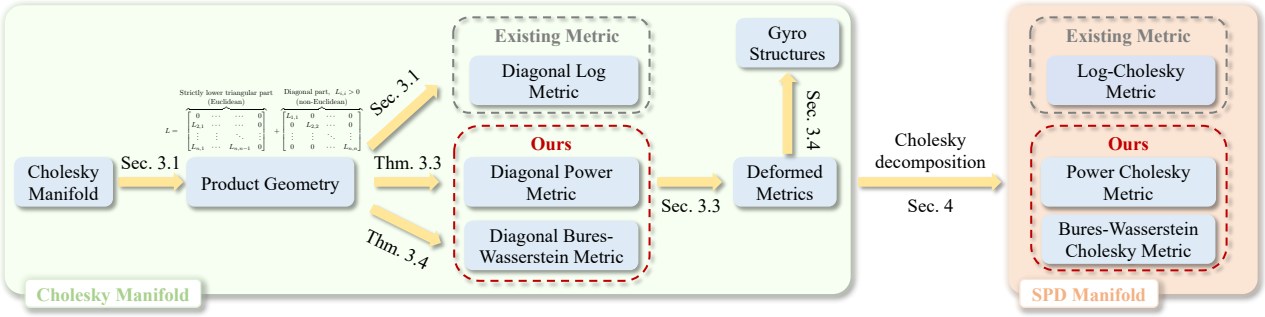

Figure A. Overview of our theoretical derivations, where L is a Cholesky matrix, *i.e.*, a lower triangular matrix with positive diagonals. Starting from existing metric on the Cholesky manifold, we reveal the product structure (Sec. 3.1), propose two new metrics (Thms. 3.3-3.4), analyze their deformations (Sec. 3.3) and gyro structures (Sec. 3.4), and finally pull them back via Cholesky decomposition to obtain the Power Cholesky Metric (PCM) and Bures-Wasserstein Cholesky Metric (BWCM) on the SPD manifold (Sec. 4).

Table A. Failure probabilities (%) of geodesics under different metrics with a small eigenvalue ϵ in $L \in \mathcal{L}^3_{++}$. An output matrix containing any INF or NAN is considered a failure. Here, DLM denotes the diagonal log metric. Experiments follow Tab. 2 in the main paper.

ϵ	DLM	$\theta = 1.5$		$\theta = 0.5$		$\theta = 0.25$		$\theta = 0.15$	
		θ-DPM	$(\theta, \mathbb{M})$-DBWM	θ-DPM	$(\theta, \mathbb{M})$-DBWM	θ-DPM	$(\theta, \mathbb{M})$-DBWM	θ-DPM	$(\theta, \mathbb{M})$-DBWM
$1e^{-1}$	0.62	0	0	0	0	0	0	0	0
$1e^{-2}$	5.70	0	0	0	0	0	0	0	0
$1e^{-3}$	51.32	0	0	0	0	0	0	0	0
$1e^{-4}$	94.34	0	0	0	0	0	0	0	0
$1e^{-5}$	99.39	0	0	0	0	0	0	0	0
$1e^{-10}$	100	0	0	0	0	0	0	0	0
$1e^{-15}$	100	0	0	0	0	0	0	0	0
$1e^{-16}$	100	0	0	0	0	0	0	0	0
$1e^{-17}$	100	0	0	0	0	0	0	0	0
$1e^{-18}$	100	0	0	0	0	0	0	0	0
$1e^{-19}$	100	0	0	0	0	0	0	0	0
$1e^{-20}$	100	0	0	0	0	0	0	0	0.002
$1e^{-21}$	100	0	0	0	0	0	0	0	0.015
$1e^{-22}$	100	0	0	0	0	0	0	0	0.25
$1e^{-23}$	100	0	0	0	0	0	0	0	2.29
$1e^{-24}$	100	0	0	0	0	0	0	0	22.78
$1e^{-25}$	100	0	0	0	0	0	0	0	86.34
$1e^{-30}$	100	0	0	0	0	0	0	0	100

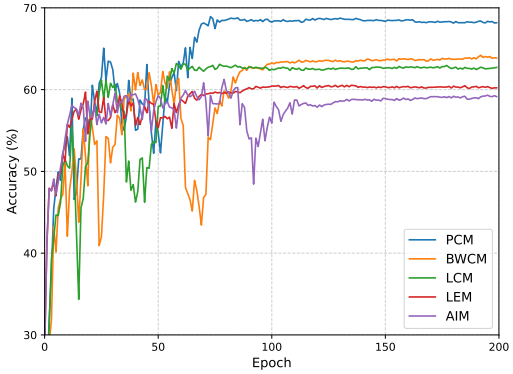

Figure B. Testing accuracy curve of SPD MLRs under different metrics on the SPDNet backbone. Here, we focus on the 3-block architecture on the HDM05 dataset.